

MECHANICAL RESPONSE OF HPFRCC IN TENSION
AND COMPRESSION AT HIGH STRAIN RATE
AND HIGH TEMPERATURE

E. Cadoni¹⁾, A.M. Bragov²⁾, A. Caverzan³⁾,
M. di Prisco³⁾, A. Konstantinov²⁾, A. Lomunov²⁾

¹⁾ **University of Applied Sciences of Southern Switzerland**
DynaMat Laboratory
Switzerland

²⁾ **State University of Nizhny Novgorod**
Research Institute of Mechanics
Russia

³⁾ **Politecnico di Milano**
Department of Structural Engineering
Italy

The mechanical response of High Performance Fibre-Reinforced Cementitious Composite (HPFRCC) has been analyzed at high strain rates and high temperature. Two experimental devices have been used for compression and tension tests: the traditional Split Hopkinson Pressure Bar for compression and the JRC-Split Hopkinson Tension Bar for tension. The HPFRCC was thermally damaged at 3 temperatures (200°C, 400°C and 600°C) in order to analyze the dynamic behaviour of this material when explosions and fires took place in a tunnel. Results show that significant peak strength increases both in tension and in compression. The post-peak strength in tension depends on the thermal damage of the material. Its strain-rate sensitivity and thermal damage have been illustrated by means of a Dynamic Increase Factor. These results show that it is necessary to implement new expression of the DIF for the HPFRCC, therefore more and more accurate and experimental studies using Kolsky–Hopkinson Bar methods are needful.

1. INTRODUCTION

The mechanical response of concrete structures subjected to impact loading and high temperature, main load conditions present in explosions and fires in tunnel, cannot be ignored in the design, but they have to be predicted and controlled starting by investigation into proper material models for cementitious composites, including strain-rate effects and thermal damage. The mechanical behaviour of cementitious composites when they are subjected to extreme temperatures, impacts or blast has still many aspects open to investigation.

As a matter of fact, a scanty information provided so far by such special equipments as the Split Hopkinson Pressure Bar (SHPB) and Split Hopkinson Tension Bar (SHTB) for very high strain rates (as in explosions) shows significant increases in peak strength. However, dynamic peak strength is not sufficient to design a structure subjected to a dynamic load. Moreover, fibre cementitious composites are often used to improve the impact resistance, preventing scabbing and fragmentation problems, due to their ability in energy absorption, but the link between the dynamic energy and the static energy absorption, its strain-rate sensitivity and thermal damage influence are not clear as yet. The work described herein focuses on the behaviour of thermally damaged High Performance Fibre-Reinforced Cementitious Composites subjected to high strain-rate in tension and compression that is presented and compared with results obtained in a static range.

2. EXPERIMENTAL PROGRAM

Compression and tension loading tests were carried out on 20 mm high, cylindrical specimens with a 20 mm diameter (see Fig. 1). The specimens subjected to tension test were pre-notched (notch = 1.5 mm) in order to prevent multiple fractures.

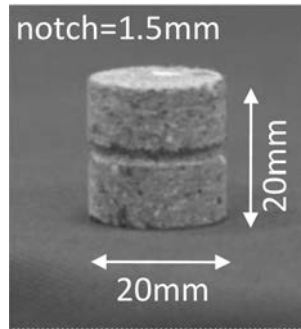


FIG. 1. Specimen for tension.

These specimens were tested under quasi-static conditions by a closed-loop electro-mechanical press and under high strain rates by a SHPB and a SHTB for compression and tension tests respectively.

2.1. Materials

The mix design of the HPFRCC material is specified in Table 1. Steel fibres are high carbon, straight fibres, 13 mm long, with a 0.16 mm diameter; their content is equal to 100 kg/m³ [1].

Table 1. HPFRCC Mix design.

	Dosage (kg/m ³)
Cement type I 52.5	600
Slag	500
Water	200
Super plasticizer	33 (l/m ³)
Sand 0–2 mm	983
Fibres ($l_f = 13$ mm; $d_f = 0.16$ mm)	100

Manufacturing process was composed by more phases. First of all, a 30 mm thick, 1.6 m wide and 0.60 m deep was cast in plane. The casting was carried out by applying a unidirectional flow in order to guarantee a certain fibre orientation. Twelve prismatic samples, 40 mm wide and 600 mm long, were sawn from the slab taking the larger side of beam samples parallel to the casting flow direction. Three specimens were tested in bending at room temperature [2–3]. Nine beam specimens, with the same geometry, were used to investigate the degradation of post-cracking residual strengths in bending after exposure to high temperatures [2–3]. From the bent specimens, several small cylinders, investigated here, were cored in the direction of tensile stresses to be tested in uniaxial tension at different loading rates. The thermal treatment of the samples was carried out in a furnace by performing thermal cycles up to three different maximum temperatures: 200, 400 and 600°C. A heating rate equal to 50°C/h was imposed up to the maximum thresholds, and then two hours of stabilization were guaranteed in order to assure a homogeneous temperature distribution within the sample volume. The temperature was then reduced with a rate of 25°C/h down to 100°C and then a cooling process at room temperature was carried out (see Fig. 2). For each cycle, three nominally identical samples were introduced into the furnace.

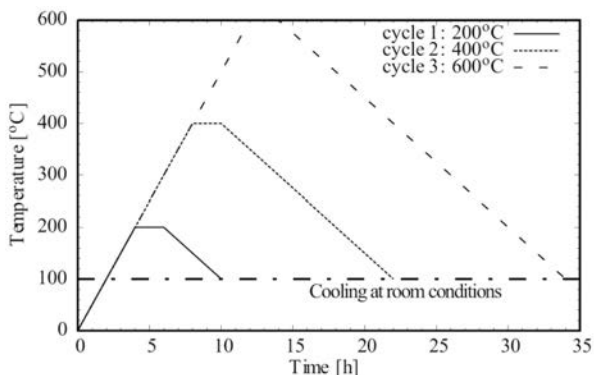


FIG. 2. Thermal cycles.

3. STATIC AND DYNAMIC TESTING SET-UPS

3.1. *Quasi-static tension and compression tests*

In order to characterize the material behaviour in the static field, several uni-axial tension tests were carried out on notched cylinders with 20 mm diameter, and 20 mm height (notch depth = 1.5 mm), glued to the press platens by means of an epoxy resin. The tests were carried out by means of close-loop electro-mechanical press INSTRON 5867, in the laboratory of Politecnico di Milano – Polo Regionale di Lecco. The press has a maximum loading capacity equal to 30 kN. Two aluminium cylinders connected to the press by a knuckle joint were used as press platens. In both cylinders, a 5 mm deep cylindrical cavity with a 22 mm diameter was made in order to increase the glued sample surface. Stroke was considered as a feedback parameter during the tests. The displacement rate imposed during the tests was equal to 5×10^{-5} mm/s up to 1.5 mm and it was progressively increased up to 10^{-3} mm/s. For each temperature (room conditions, 200°C, 400°C and 600°C), three samples were tested. The compression tests were carried out by means of an electro-mechanical press INSTRON 8562. The aluminium press platens were replaced by two steel platens. A thin layer of stearic acid was placed between samples and platens in order to reduce the friction.

3.2. *Dynamic tension tests*

The dynamic direct tension tests were performed using a modified Hopkinson Bar called JRC-Split Hopkinson Tensile Bar (JRC-SHTB) [4–5], installed in the DynaMat laboratory of the University of Applied Sciences of Southern Switzerland (SUPSI) of Lugano (Fig. 3).



FIG. 3. Dynamic direct tensile testing set-up.

The JRC-SHTB consists of two circular aluminium bars, called input and output bars, having the lengths respectively of 3 m and 6 m, with a diameter of 20 mm, to which the HPFRCC specimen is glued using an bi-component epoxy resin. The input bar is connected with a high-strength steel pretension bar with a length of 6 m and a diameter of 12 mm. The pretension bar is used for the generation of the pulse loads. The hydraulic actuator placed at the end of the system is directly connected to one end of the pretension bar. The pretension bar is clamped at the other end by a blocking device. Pulling the pretension bar, the elastic energy is stored in it. Rupturing the fragile bolt in the blocking device, a tensile mechanical pulse of 2.4 ms duration is produced. It propagates along the input and output bars leading to fracture of the specimen.

The pulse propagates along the input bar with the elastic wave velocity C_0 , during the propagation phase the wave shape remains constant. When the incident pulse (ε_I) reaches the HPFRCC specimen, part of it (ε_R) is reflected by the specimen whereas another part (ε_T) passes through the specimen propagating into the output bar, as shown in Fig. 4. The relative amplitudes of the incident, reflected and transmitted pulses, depend on the mechanical properties of the specimen. Strain-gauges glued on the input and output bars of the device are used for the measurement of the elastic deformation (as a function of time), created on both half-bars by the incident/reflected and transmitted pulses, respectively. In Fig. 4 the raw signals measured on the input and out-

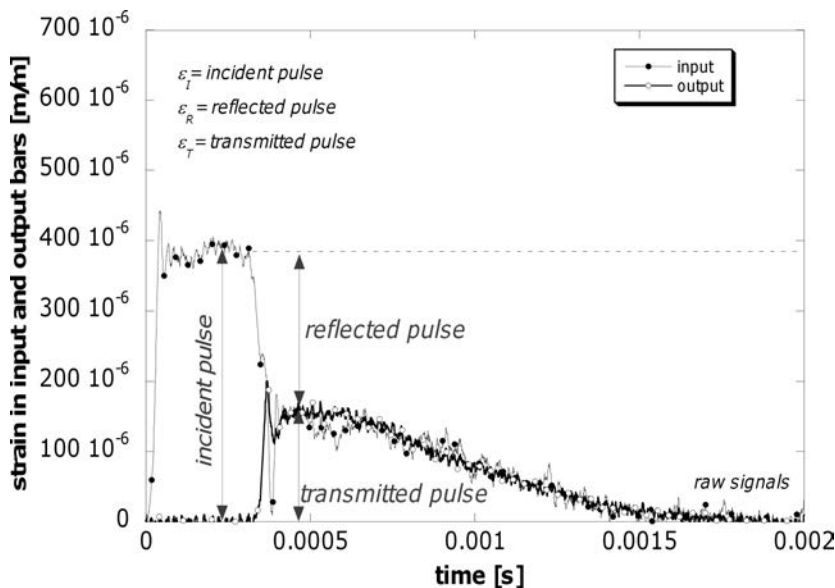


FIG. 4. Signals measured on the input and output bar versus time curves of HPFRCC.

put bars of the JRC-SHTB are shown. We can observe the clean resolution of incident, reflected and transmitted pulses, the sharp rise time of the incident pulse of the order of 30 μs , and the nearby constant amplitude of the incident pulse. Moreover during the fracture process the specimen is subjected to the load equilibrium because the signals $(\varepsilon_I + \varepsilon_R)$ and ε_T are equal.

By using the theory of the elastic wave propagation in bars, and the well substantiated assumption of specimen equilibrium attainment, the stress (Eq. (3.1)) and strain (Eq. (3.2)) as well as the displacement (Eq. (3.3)) and the strain-rate (Eq. (3.4)) in the specimen can be calculated [4–5]:

$$(3.1) \quad \sigma(t) = E_0 \frac{A_0}{A} \varepsilon_T(t),$$

$$(3.2) \quad \varepsilon(t) = -\frac{2 \cdot C_0}{L} \int_0^t \varepsilon_R(t) dt,$$

$$(3.3) \quad \delta(t) = -2 \cdot C_0 \int_0^t \varepsilon_R(t) dt,$$

$$(3.4) \quad \dot{\varepsilon}(t) = -\frac{2 \cdot C_0}{L} \varepsilon_R(t),$$

where E_0 is the elastic modulus of the bars; A_0 their cross-sectional area; A is the specimen cross-section area; L is the specimen gauge length; C_0 is the sound velocity of the bar material; t is time.

3.3. Dynamic compression tests

The dynamic compression tests were performed using a Split Hopkinson Pressure Bar (SHPB), installed in the Dynamic Testing of Materials Laboratory of the Research Institute of Mechanics-Nizhny Novgorod University (Russia), which consists of an input (2) and an output (5) bar with the specimen (4) sandwiched between them, what is schematically shown in Fig. 5. When the strike bar (1) impacts onto the input bar, a compressive incident wave $\varepsilon_I(t)$ travels along the input bar. Once it reaches the specimen, a reflected wave $\varepsilon_R(t)$ and a transmitted wave $\varepsilon_T(t)$ are generated, propagating along the input and output bar respectively. According to the one-dimension wave propagation theory, the forces and particle velocities/displacements at the two faces of specimen can be determined by those three waves recorded.

In Fig. 5a the Lagrangian graph describing the strain history of the two bars is also shown. In Fig. 6 the signals of the input and output of a dynamic

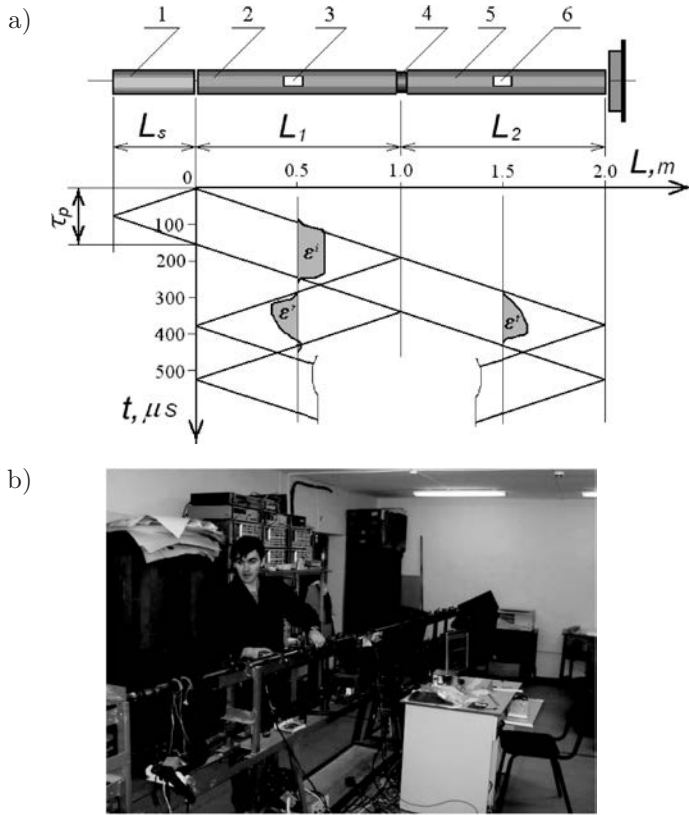


FIG. 5. Dynamic compression testing set-up: a) scheme and Lagrangian graph; b) view.

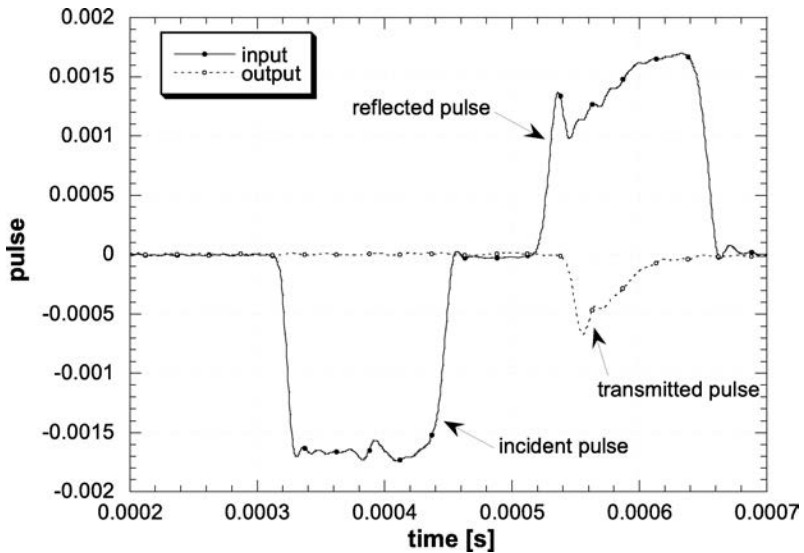


FIG. 6. Signals measured on the input and output bars versus time curves of HPRCC.

compression tests of HPFRCC specimen are shown. It can be observed that the failure of the specimen is reached just in the first loading cycle. By comparing Fig. 4 and Fig. 6 it can be noted that in the case of compression, the time necessary to bring the specimen at failure is about 100 μs , while in the case of tension, more than 1.5 ms is needed.

4. RESULTS AND DISCUSSION

The comparison between the tensile and compression behaviour at high strain rates of HPFRCC with different thermal damage is here presented. The tests were performed with a strain rate of 150 s^{-1} in tension and 500 s^{-1} in compression. The results are summarized in Table 2.

Table 2. Dynamic results.

Temperature [$^{\circ}\text{C}$]	Compression strength [MPa]	DIF_C (500 s^{-1})	Tensile strength [MPa]	DIF_T (150 s^{-1})
20	117.4 \pm 18	2.20	24.96 \pm 2.3	2.85
200	162.0 \pm 25	2.58	26.08 \pm 1.0	2.61
400	134.4 \pm 21	3.07	25.28 \pm 3.9	2.27
600	132.0 \pm 30	2.45	32.49 \pm 1.5	5.40

High temperature exposure influences both the static and dynamic material behaviour. The comparison between static and dynamic tensile stress versus displacement curves are shown in Fig. 7. In order to highlight the first linear elastic branch and post peak behaviour close to the peak, a detail of the peak zones is plotted. Observing Fig. 7 it is possible to note that the behaviour changes as a function of the exposition to high temperature. As in a static tests, specimens cured at room conditions show a post-peak stress plateau up to a displacement of 0.4 mm. The constant stress plateau decreases with temperature growth. At 600 $^{\circ}\text{C}$ the behaviour is significantly changed, becoming weakly softening in the post-peak region. At this velocity, the peak increases with the exposition to high temperature as well as the post-peak strength decreases to disappear for higher temperatures.

By observing the fracture surface of the specimen it is evident as the failure type has changed (Fig. 7). In the first case (Fig. 7a), the observable hole in the specimen demonstrates the fibre pullout process occurrence, while in the second one (Fig. 7b) all the fibres are broken.

In Fig. 8 the stress versus displacement curves of the compression test, both in quasi-static and dynamic condition, are shown. The HPFRCC exhibits an increase of strength with increasing strain-rate, also in compression

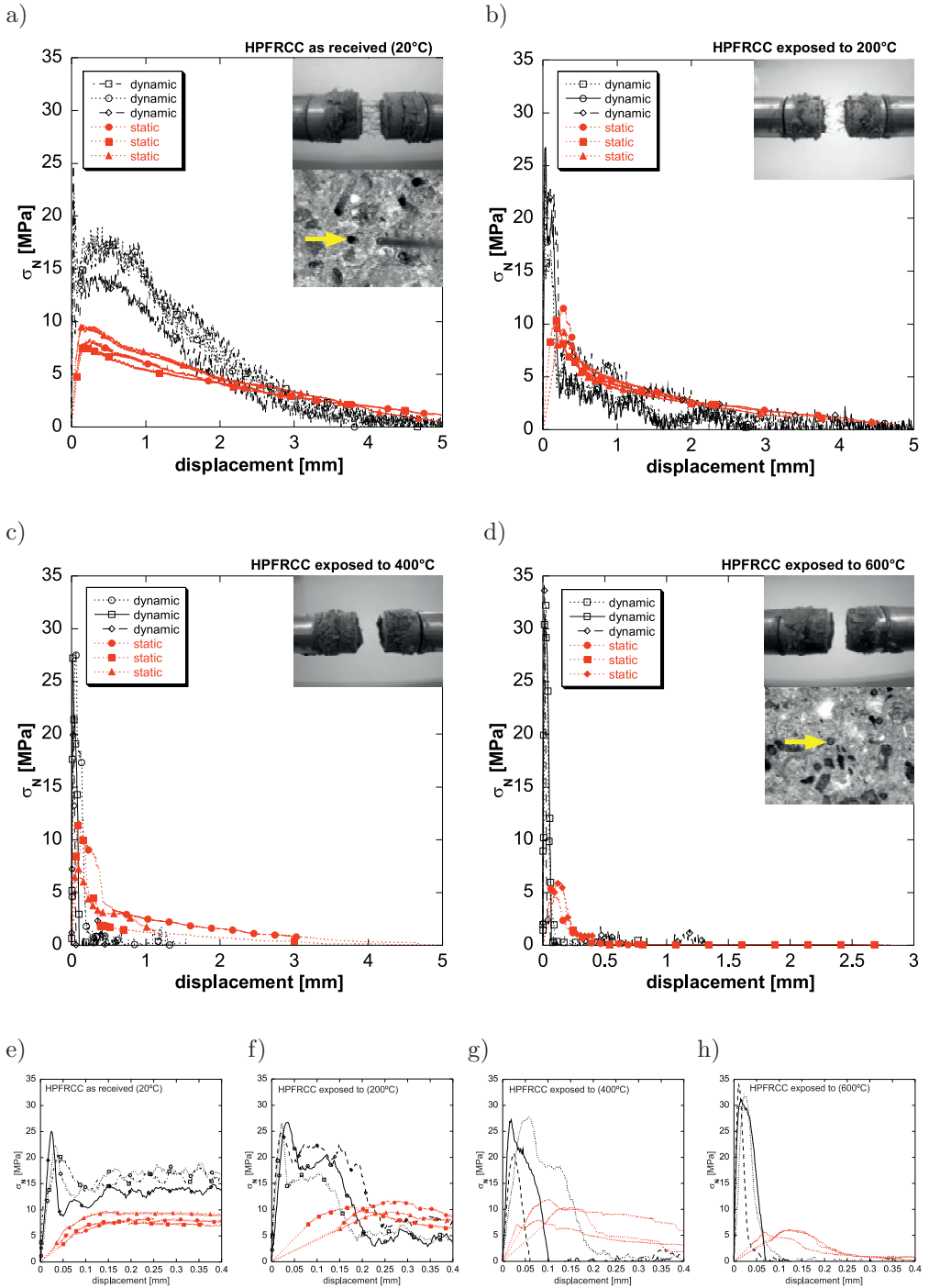


FIG. 7. Comparison of the tension quasi-static and dynamic stress vs. displacement curves of the tests at different temperature: a) 20°C; b) 200°C; c) 400°C; d) 600°C.

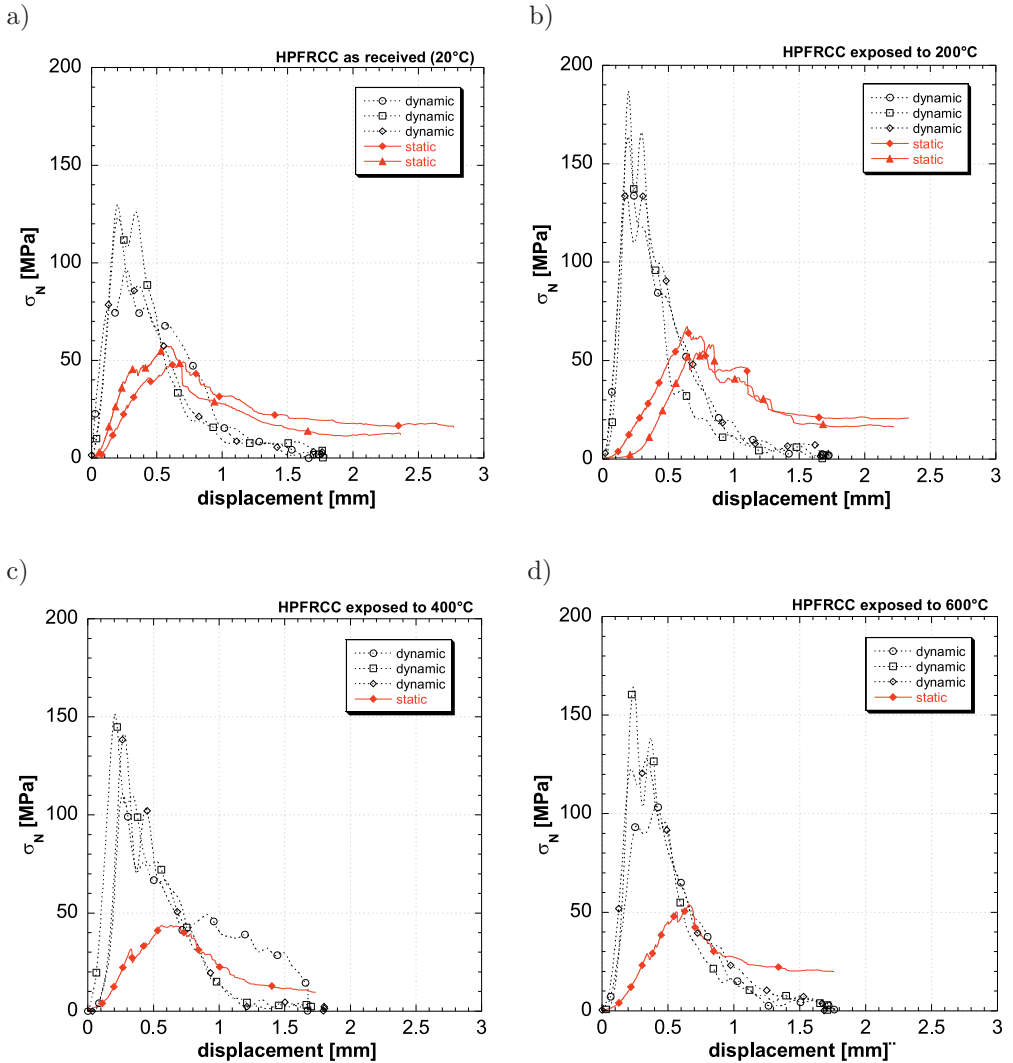


FIG. 8. Compression quasi-static and dynamic stress vs. displacement curves of the tests at different temperatures: a) 20°C; b) 200°C; c) 400°C; d) 600°C.

4.1. Dynamic Increase Factor

Dynamic Increase Factor (DIF) has been extensively used in order to quantify the strain-rate effects for concrete, and some expressions of the DIF for the tensile and compression have been proposed. However, no expressions of DIF are available for HPFRCCs due to the lack of experimental results. Often these expressions are generated by experimental data obtained by different experimental

techniques, as the tensile strength obtained from direct or indirect tension tests (splitting, spalling, bending, etc.).

The most comprehensive model for predicting the strain-rate enhancement of concrete is presented by the CEB Model Code [6]. It provides specifications for the DIF for concrete in tension and compression.

The suggested expression are the following:

$$(4.1) \quad \text{DIF}_{\text{CEB,tension}} = \begin{cases} 1 & \dot{\epsilon}_d \leq \dot{\epsilon}_s, \\ \left(\frac{\dot{\epsilon}_d}{\dot{\epsilon}_s}\right)^{1.016\alpha} & \dot{\epsilon}_s < \dot{\epsilon}_d \leq 30 \text{ s}^{-1}, \\ \gamma \left(\frac{\dot{\epsilon}_d}{\dot{\epsilon}_s}\right)^{0.33} & \dot{\epsilon}_d > 30 \text{ s}^{-1}, \end{cases}$$

with $\gamma = 10^{(7.11\alpha-2.33)}$; $\alpha = 1/(10+6f_c/10)$; f_c is the static compressive strength in MPa, and $\dot{\epsilon}_s = 3 \cdot 10^{-6} \text{ s}^{-1}$.

$$(4.2) \quad \text{DIF}_{\text{CEB,compression}} = \begin{cases} 1 & \dot{\epsilon}_d \leq \dot{\epsilon}_s, \\ \left(\frac{\dot{\epsilon}_d}{\dot{\epsilon}_s}\right)^{1.026\alpha} & \dot{\epsilon}_s < \dot{\epsilon}_d \leq 30 \text{ s}^{-1}, \\ \mu \left(\frac{\dot{\epsilon}_d}{\dot{\epsilon}_s}\right)^{0.33} & \dot{\epsilon}_d > 30 \text{ s}^{-1}, \end{cases}$$

with $\mu = 10^{(6.156\alpha-2)}$; $\alpha = 1/(5 + 9f_c/10)$; f_c is the static compressive strength in MPa, and $\dot{\epsilon}_s = 30 \cdot 10^{-6} \text{ s}^{-1}$.

The prediction has been carried out by assuming a perfect uncoupling between thermal damage and strain effect, a compressive strength variable, with the temperature on the basis of performed experimental tests and a variation with high strain-rate according to CEB formulation. This prediction is indicated in Fig. 9 as ‘‘CEB’’ DIF: the comparison with experimental results is shown in Fig. 9.

The CEB formula overestimates the compression strength comparing those actually recorded in the tests for all four exposure temperatures. The overestimation may be due to the effect of fibres and their distribution. The analyzed material has fibres oriented in the direction of the load. As reported in [7] for the tension tests, increasing of the temperature the DIF does not significantly change up to the maximum temperature of 400°C, DIF is close to 2.5 till 400°C and suddenly goes up to 5.5 at 600°C. Looking at the results obtained in the compression tests, increasing of the temperature the DIF increase up to a maximum of 3 for 400°C, and slightly lower value than 2.5 for 600°C.

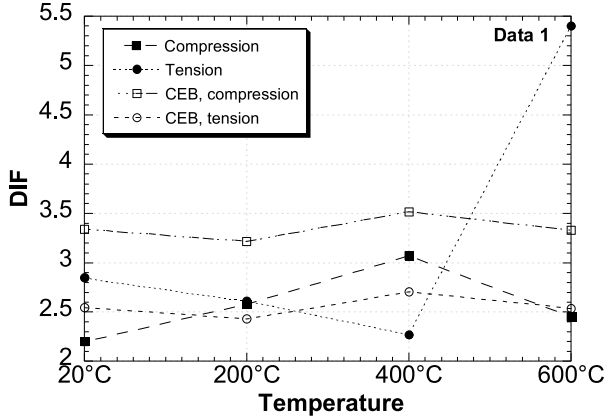


FIG. 9. Comparison between the experimental and CEB DIF at different temperature.

The CEB formulations were developed for concrete and its suboptimal estimate for other fibre-reinforced material; in a future paper, a new DIF formulation for HPFRCC will be proposed.

5. CONCLUDING REMARKS

The following remarks can be drawn from this study on the tension and compression behavior of HPFRCC under high strain-rates and high temperatures.

- The undamaged material showed a stress plateau in region close to the peak strength. This plateau was observed at different strain rates. Increasing the strain rate from 10^{-6} to 150 s^{-1} the stress plateau grows from 8.5 to 15 MPa. This stress plateau seems to be rate-sensitive as well as the tensile strength.
- The material is strain hardening at room temperature in tension and under quasi-static loads; high temperature exposure up to 400°C does not decrease the tensile peak strength, slightly decreases the ductility before the single crack localization and progressively decreases the post-peak fracture energy; an abrupt peak strength decrease can be observed at 600°C .
- At high strain rate, the dynamic factor related to tensile peak strength is increased by high temperature exposure, passing from about 2.5 up to 400°C to more than 5 at 600°C at a strain rate of 150 s^{-1} .
- The compression strength increases with increasing the strain rate, obtaining at least two times the static value. This increase is influenced by the temperature.
- The dynamic compression strength could be influenced by the fibres, which are parallel to the load direction in the samples tested. New experimental

tests will be carried out on plain material in order to investigate the fibre influence.

ACKNOWLEDGMENT

The Authors are grateful to Matteo Dotta and Daniele Forni of the University of Applied Sciences of Southern Switzerland, Matteo Colombo and Giulio Zani of the Politecnico di Milano for their precious collaboration in the the laboratory tests. The research was partially financed by the project ACCIDENT ID 7629770 in the frame of INTERREG IT/CH 2006-2013 program.

Moreover a special acknowledgements goes to the Scientific & Technological Cooperation Programme Switzerland-Russia for the financial support of the Utilisation of Specific Infrastructure Projects called “Dynamic behaviour of materials for industrial applications”. Russian part of investigations was partially financed by RFBR (Grant 10-01-00585).

REFERENCES

1. E. CADONI, A. CAVERZAN and M. DI PRISCO, *Dynamic behaviour of HPFR cementitious composites*, [in:] Ultra-High Performance Concrete, Fehling, Schmidt and Stürwald [Eds.], Proceedings of the 2nd International Symposium on Ultra-High Performance Concrete, Kassel, Heft 10, Structural Materials and Engineering Series, Kassel University Press, 2008, 743–750.
2. A. CAVERZAN, M. COLOMBO and M. DI PRISCO, *High performance steel fibre reinforced concrete: Residual behaviour at high temperature*, [in:] Proceedings of 2nd Workshop on Performance, Protection and Strengthening of Structures under Extreme Loading PROTECT 2009, Hayama, Japan, 2009, on CD ROM.
3. A. CAVERZAN, *High Strain-Rate Uniaxial Tensile Constitutive Behaviour in Fibre Reinforced Cementitious Composites*, Ph.D. Thesis, Politecnico di Milano, 2010.
4. E. CADONI, G. SOLOMOS and C. ALBERTINI, *Mechanical characterization of concrete in tension and compression at high strain-rate using a modified Hopkinson bar*, Magazine of Concrete Research, **61**, 3, 221–230, 2009.
5. E. CADONI, A. MEDA and G. A. PLIZZARI, *Tensile behavior of FRC under high strain-rate*, Materials and Structures, **42**, 9, 1283–1294, 2009.
6. Comité Euro-International du Béton), CEB-FIP Model Code 1990, Redwood Books, Trowbridge, Wiltshire, 1993, UK.
7. A. CAVERZAN, E. CADONI and M. DI PRISCO, *Behaviour of advanced cementitious composites under dynamic loading and fire*, In Proc. of International Workshop on Structures Response to Impact and Blast, Haifa, Israel, 15–17 November 2009.